Cell Reports, Volume *37*

Supplemental information

Anti-SARS-CoV-2 antibodies elicited by COVID-19 mRNA vaccine exhibit a unique glycosylation pattern

Inbal Farkash, Tali Feferman, Noy Cohen-Saban, Yahel Avraham, David Morgenstern, Grace Mayuni, Natasha Barth, Yaniv Lustig, Liron Miller, Dror S. Shouval, Asaf Biber, Ilya Kirgner, Yishai Levin, and Rony Dahan

Supplementary Figures

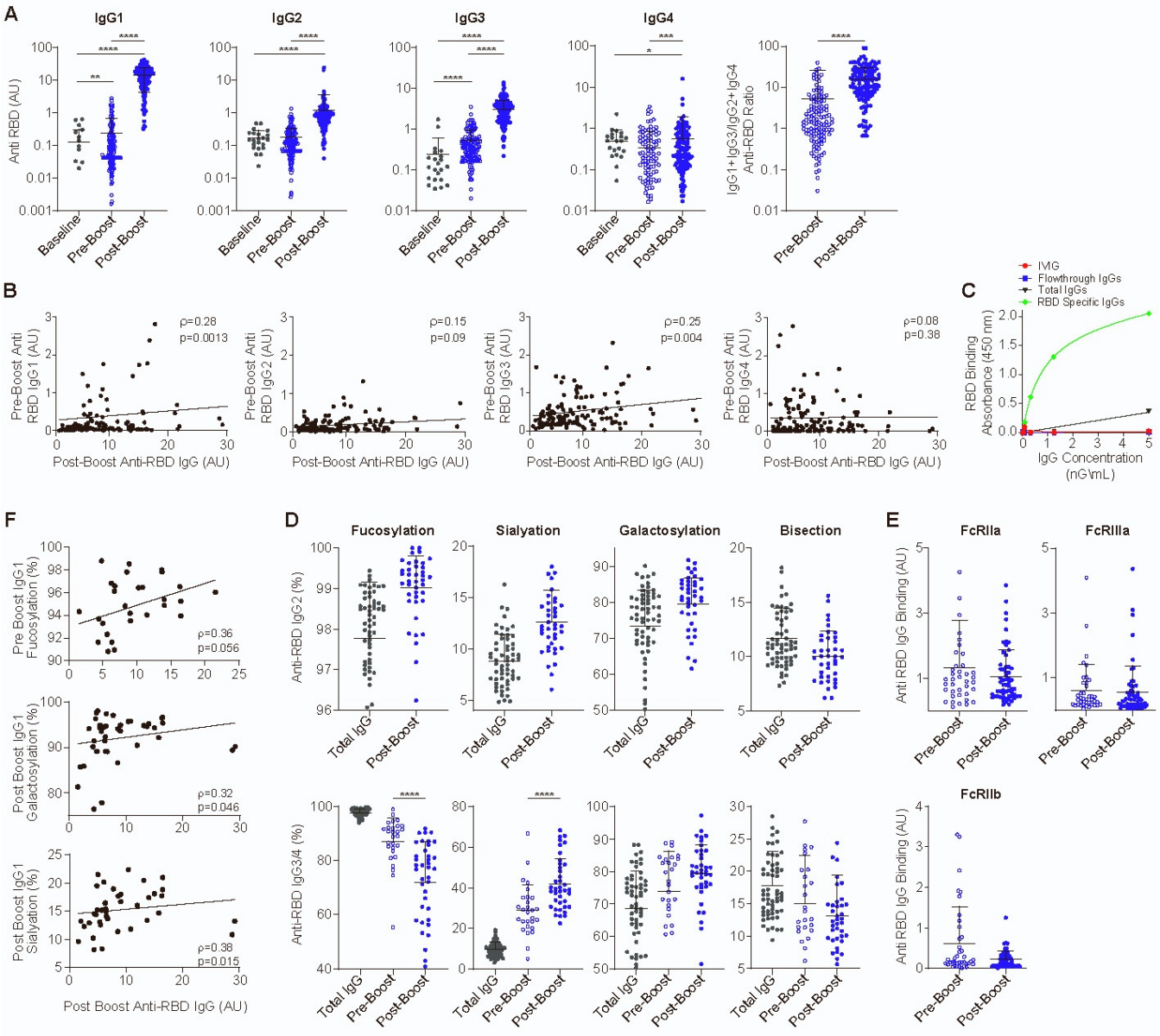

Supplementary Figure 1. Anti-RBD IgG response, subclass trajectory, Fc glycosylation patterns and effector function following the BNT162b2 vaccine. Related to Figure 1**. A** – Anti-RBD IgG subclass distribution following the first and second vaccine doses (N=127). IgG subclasses were determined for each individual serum sample. These levels were then used to calculate IgG1+IgG3/IgG2+IgG4 ratios. **B** – Correlation of post-boost anti-RBD overall IgG titers to pre-boost IgG response, by subclass. Non-parametric Spearman's correlation was used. **C** – Isolation of RBD-specific IgGs from plasma samples from vaccinated individuals. Total IgGs and anti-RBD IgGs were prepared from plasma samples obtained after each vaccine dose as described in Methods. To determine RBD binding or its absence, total IgGs, unbound flow-through IgGs and eluted RBD-specific IgGs were subjected to an RBD binding ELISA assay. Purification of representative sample is shown. **D** – Fc glycosylation patterns in anti-RBD IgG2 and IgG3/4 and in total IgGs (as reference) from vaccinated individuals. Because there was no anti-RBD IgG2 response following the first vaccine dose, only total IgGs (n=59) and post-boost anti-RBD IgG2 glycosylations (n=39) were detected and shown. Detected pre-boost IgG3 glycosylations, n=28. **E** – FcγR and C1q binding of RBD-specific IgGs from vaccinated individuals, a (pre-boost, n=39; post-boost, n=59). **F** – RBD-specific IgG1 glycosylation patterns associated with overall IgG response, as determined by the non-parametric Spearman's correlation. Shown are glycosylation patterns that were in significant correlation with overall anti-RBD IgG response. Pre-boost IgG1 fucosylation, n=28; post-boost IgG1 glycosylations, n=39.

Data are presented as scatter plots indicating individual measurements (dots); black line represents the mean; error bars represent SD. Unpaired two-sided Mann-Whitney *U* test was used to evaluate differences between groups.

*P < 0.05, **P < 0.01, ***P < 0.001, ****P < 0.0001.

A B

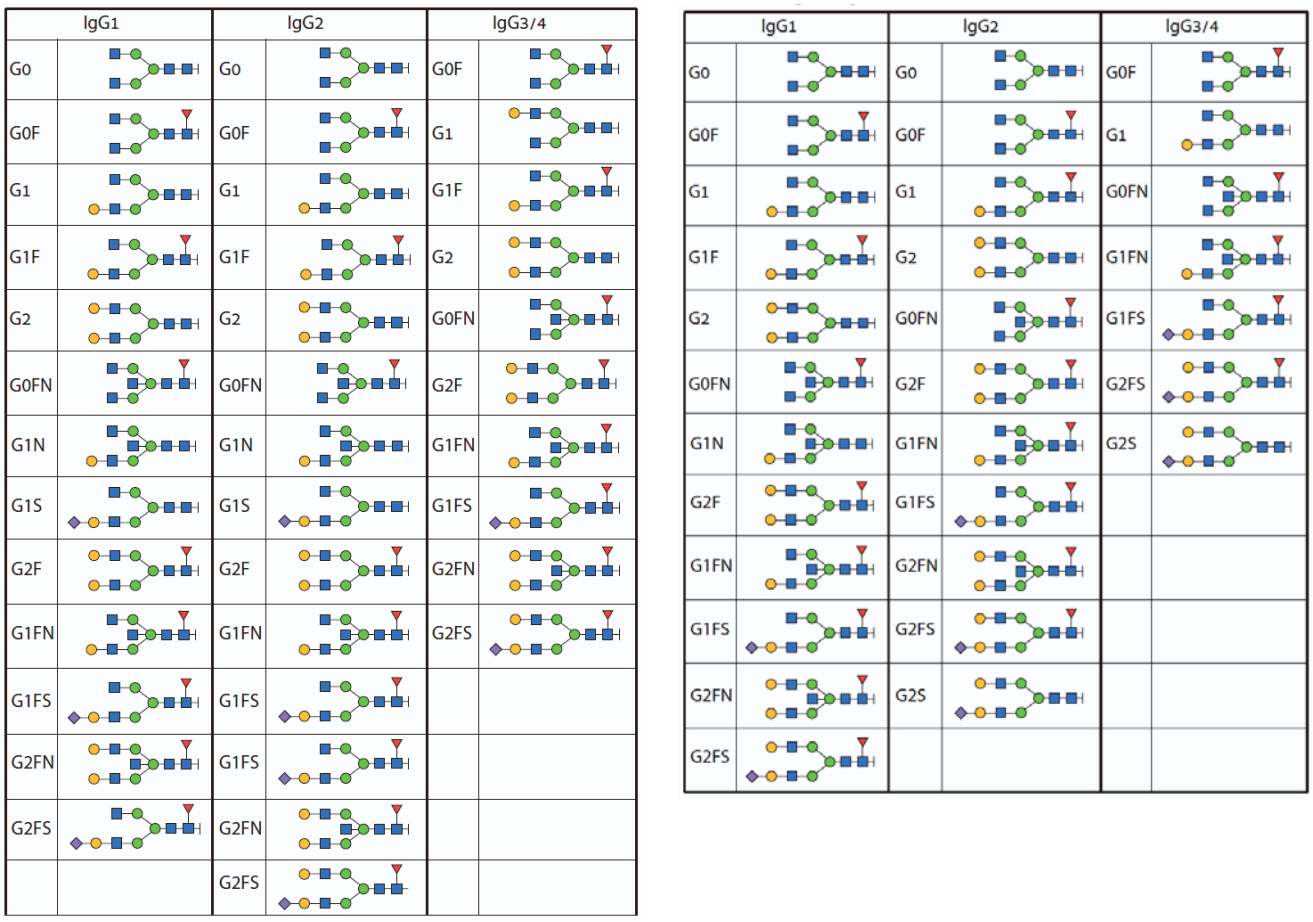

Supplementary Figure 2. Related to Figure 1F. Detected attached Fc glycans by mass spectrometry. A list of glycoforms that were detected and quantified for each IgG subclass from total IgG preparation (left) or RBD-specific purified IgG (right) obtained from sera samples.

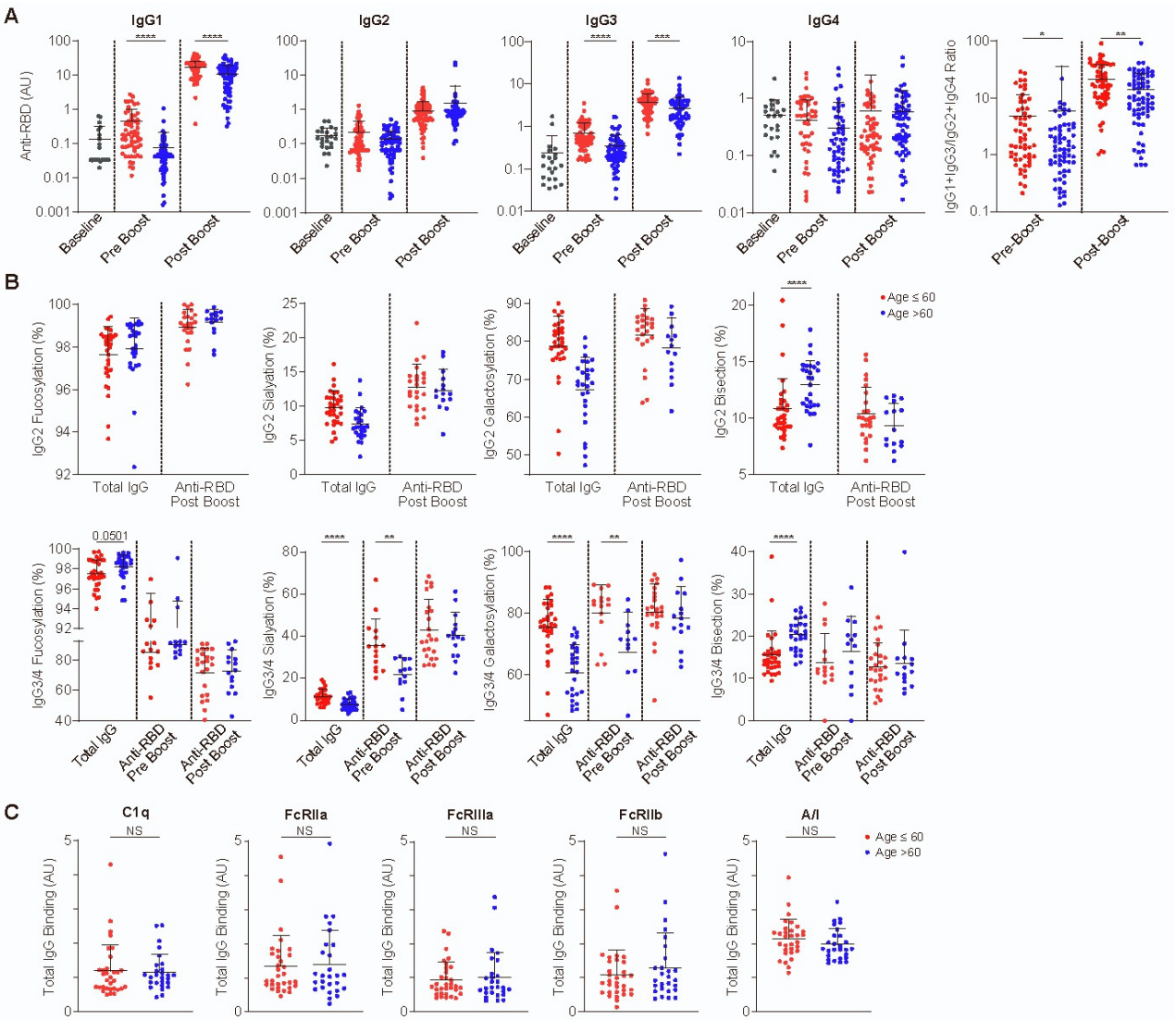

Supplementary Figure 3. Related to Figure 2**. Age-dependent structural and functional responses of anti-RBD IgG.** **A** – Age-dependent anti-RBD IgG subclass distribution following the first and second vaccine doses. IgG subclasses were determined for each individual serum. These levels were then used to calculate IgG1+IgG3/IgG2+IgG4 ratios (pre-boost: age≤ 60, n=60; age>60, n=67; post-boost: age≤ 60, n=60; age>60, n=67). **B** – Age-dependent Fc glycosylation patterns in IgG2, IgG3/4 and total IgG from vaccinated individuals. Total IgGs: age≤ 60, n=32; age>60, n=27; pre-boost IgG3: age≤ 60, n=15; age>60, n=13; post-boost IgG2 and IgG3: age≤ 60, n=24; age>60, n=15. **C** – Binding of total IgGs to FcγRs and C1q. Binding to activating vs inhibitory FcγR ratio was as described above. Age≤ 60, n=32; age>60, n=27. Data are presented as scatter plots indicating individual measurements (dots); black line represents the mean; error bars represent SD. Unpaired two-sided Mann-Whitney *U* test was used to evaluate differences between groups.
*P < 0.05, **P < 0.01, ***P < 0.001, ****P < 0.0001.

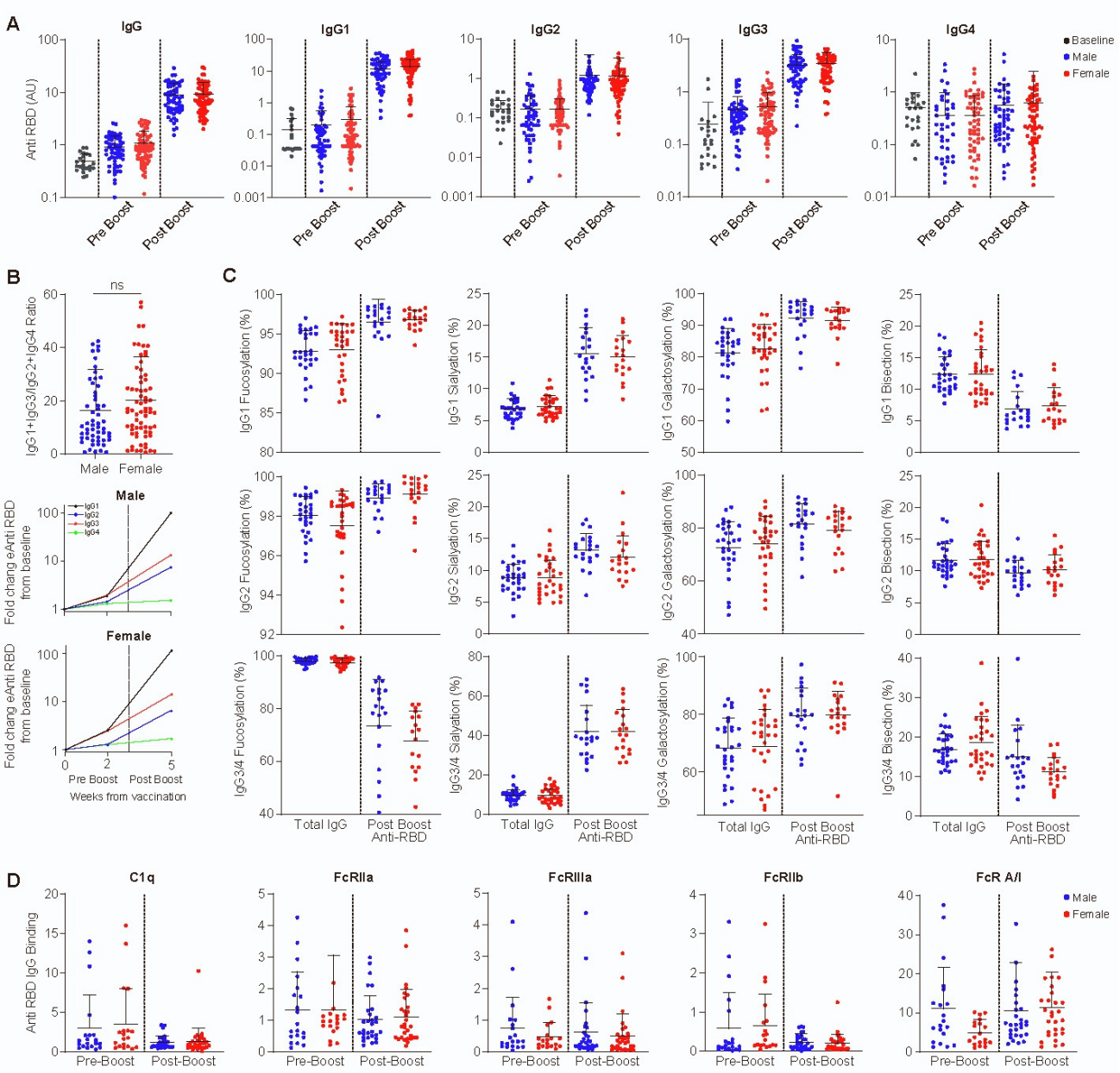

Supplementary Figure 4. Related to Figure 2. **Sex is not associated with an altered IgG response to the vaccine. A** – Anti-RBD total IgG and IgG subclass distribution following the first and second vaccine doses are not sex-dependent. IgG subclasses were determined from each individuals serum sample, see methods section. Male n=56, Female n=71. **B** – (IgG1+IgG3)/(IgG2+IgG4) ratios of anti-RBD IgG and anti-RBD IgG subclass trajectories in males (n=56) and females (n=71). Values of each subclass were used to calculate IgG1+IgG3/IgG2+IgG4 ratios. **C** – Fc glycosylation patterns of total IgGs and post-boost RBD-specific IgG1, IgG2 and IgG3/4. Total IgG: male, n=29; female, n=30; post-boost anti-RBD IgG: male, n=20; female, n=19. **D** - Binding of RBD-specific IgGs to FcγRs and C1q. Binding to each receptor was determined by ELISA at pre-boost (males n=20, females, n=19) and post-boost (males, n=29, females, n=30). Ratios between RBD-specific IgG binding to activating and inhibitory receptors were determined as described above.

Data are presented as scatter plots indicating individual measurements (dots); black line represents the mean; error bars represent SD. Unpaired two-sided Mann-Whitney *U* test was used to evaluate differences between groups.

*P < 0.05, **P < 0.01, ***P < 0.001, ****P < 0.0001.

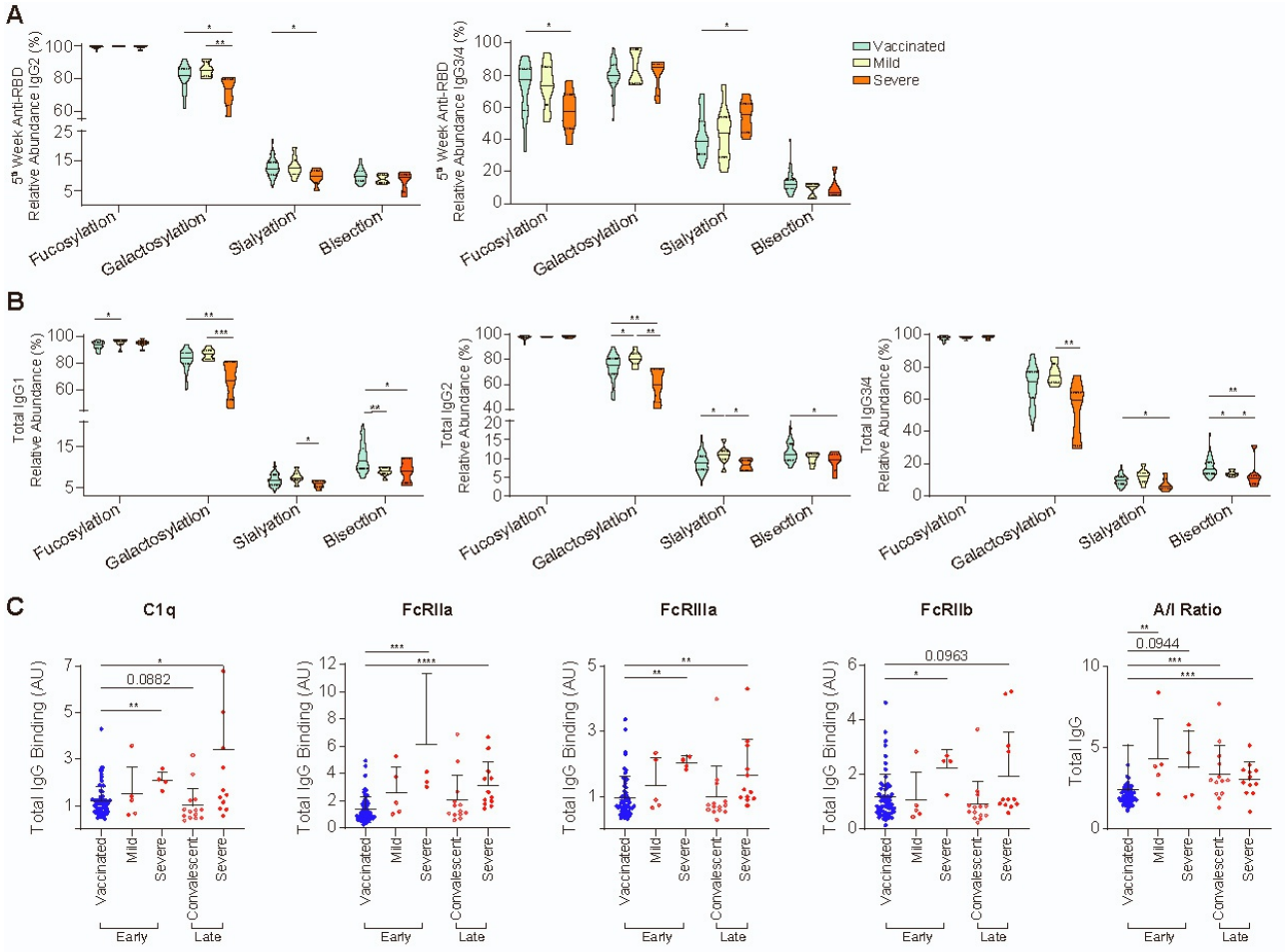

Supplementary Figure 5. Related to Figure 3. **Different anti-RBD IgG responses in vaccinated individuals vs. COVID-19 patients**. A – Distinct patterns of Fc glycosylation in anti-RBD IgG2 and IgG3/4 observed 5 weeks after vaccine or COVID-19 diagnosis (vaccinated, n=39; mild patients, n=8; severe patients, n=6. RBD-specific IgGs were isolated and Fc glycan structure was determined by mass spectrometry. Data are presented as violin plots with solid lines representing median and dotted lines upper and lower quartiles. **B** – Distinct patterns of subclass-specific Fc glycosylation, as determined by mass spectrometry, in total IgGs from vaccinated individuals and COVID-19 patients at 5 weeks from diagnosis (vaccinated, n=39; mild, n=5; severe, n=4). Data are presented as violin plots with solid lines representing median and dotted lines upper and lower quartiles. **C** - Binding of total IgGs to FcγR and C1q in severe COVID-19 patients, mild patients and vaccinated individuals (vaccinated, n=59; early mild, n=5; early severe, n=4; late mild, n=14; late severe n=12).

Unless otherwise mentioned, data are presented as scatter plots indicating individual measurements (dots); black line represents the mean; error bars represent SD. Unpaired two-sided Mann-Whitney *U* test was used to evaluate differences between groups.

*P < 0.05, **P < 0.01, ***P < 0.001, ****P < 0.0001.

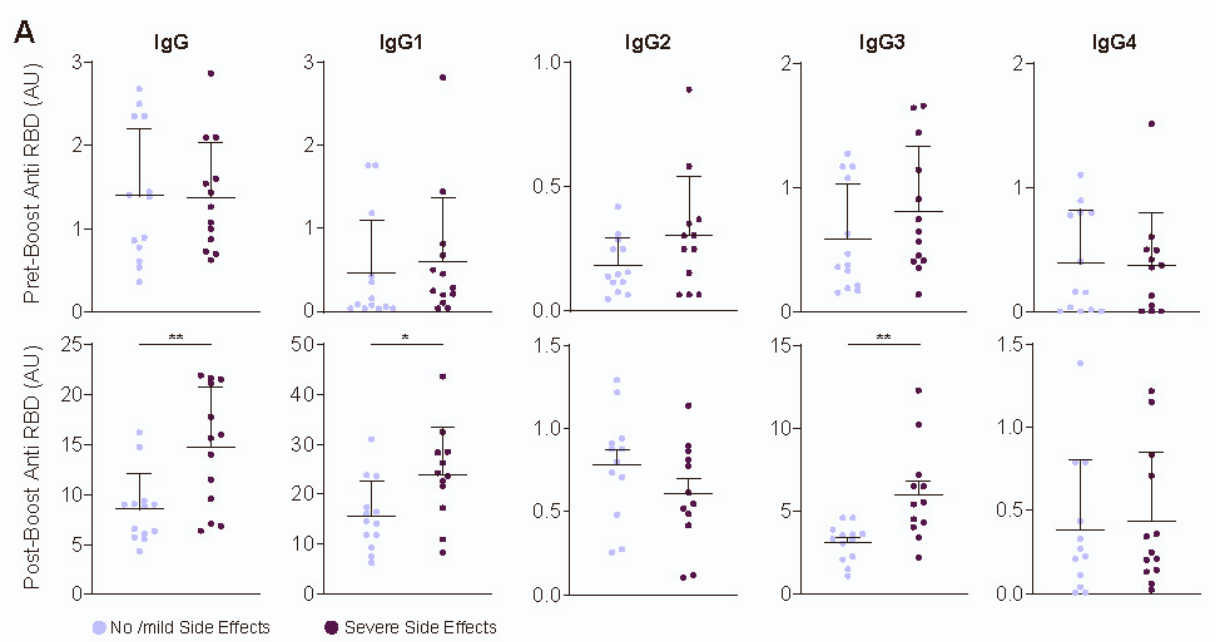

Supplementary Figure 6. Related to Figure 5. **Additional characteristics of the Anti-RBD IgG response to the BNT162b2 mRNA vaccine**. **A**- Age and sex matched analysis of Anti-RBD IgG and subclass composition by adverse event severity, as determined by ELISANo side effects, n=13; severe side effect, n=13.
Data are presented as scatter plots indicating individual measurements (dots); black line represents the mean; error bars represent SD. Unpaired two-sided Mann-Whitney *U* test was used to evaluate differences between groups.
*P < 0.05, **P < 0.01, ***P < 0.001, ****P < 0.0001.